

HEAVY QUARK PRODUCTION IN K_T FACTORIZATION APPROACH AT LHC ENERGIES

Yu.M. Shabelski¹, A.G. Shuvaev¹, I.V. Surnin^{1,2}

¹Petersburg Nuclear Physics Institute, Kurchatov National Research Centre
Gatchina, St. Petersburg 188300, Russia

²Saint Petersburg State University, St.-Petersburg, Russia

E-mail: shabelsk@thd.pnpi.spb.ru
E-mail: shuvaev@thd.pnpi.spb.ru
E-mail: surnin.ivan@mail.ru

Abstract

A new version of the k_T factorization approach is formulated for the high energy heavy quark production. The results are in reasonable agreement with the experimental data at LHC energies.

1 Introduction

The description of hard interactions in hadron collisions is carried out in the perturbative QCD on the basis of parton distribution functions. The hard cross section results from the convolution of the incident partons' densities with the squared sub-process amplitude of their scattering. While some phenomenology is needed to find the first the latter is evaluated perturbatively. The simplest and most popular way to do it is the parton model.¹⁻³

The parton model rests upon the collinear approximation, according to which the partons participating in the scattering stem from the subsequent emission off the colliding hadrons. The angles at which they are emitted, or their transverse momenta, increase for each consecutive emission reaching the top value for the partons involved in the hard subprocess. The evolution of the parton distribution as a function of maximal allowed transverse momentum square Q^2 is governed by DGLAP equation that collect the large terms $\log Q^2/\mu^2$ for a certain scale μ^2 .⁴

The value Q^2 is supposed to be negligible compared to the transverse momenta of the heavy quarks in the conventional parton model. As a virtuality of the emitted partons is of the order of their transverse momenta in the leading logarithmic approximation they are treated as mass shell particles with purely longitudinal momenta. The heavy quarks are produced therefore back to back so that the total transverse momentum of the quark-antiquark pair is always zero. The virtuality of the incoming partons is taken into account only through Q^2 dependence of the structure functions. A more elaborated kinematics, in particular non vanishing pair transverse momentum, requires to go beyond the leading order (LO) of the parton model.

There is another parameter that becomes significant for the very high energy, $\log 1/x$, where x is the total momentum fraction carried by a parton. The small x is the region where BFKL dynamics works.^{5,6} An effective approach to the dynamics for $x \ll 1$ and large Q^2 is k_T factorization method,^{7–10} in which the partons are assumed to be virtual like in the Feynman diagrams. The basic difference from the conventional parton model is that the partons in this approach poses an intrinsic transfer momentum, which is not more neglected. The leading order of the k_T factorization embodies not only LO of the parton model but an essential part of the next to leading corrections, mostly those coming from the extended subprocess kinematics. The method of k_T factorization gives a reasonable description of the experimental data up to Tevatron collider energy.^{11–13} The new data on the charm and beauty production at the LHC energies opens a new opportunity to compare the theory with the experiment at the high energies up to $\sqrt{s} = 13$ TeV.

The heavy quark production at the high energy goes mainly via gluon fusion in the small x region. Here there are no reasons to neglect the gluon transverse momentum q_T with respect to the relative momentum of the quark pair p_T . At the very high energies and $p_T \gg m_Q$, m_Q is the quark mass, the main contribution to the cross sections comes from the momenta $q_T \sim p_T$,¹⁴ which points to the k_T factorization as a natural tool to deal with it.

In the present paper we give the description of p_T distributions of the charm and beauty mesons produced at various rapidity intervals, keeping in mind that the meson distributions are similar to the heavy quark distributions ¹.

¹In e^+e^- annihilation the charm and beauty mesons are produced via fragmentation of the incident heavy quark, so the outcome meson spectra are softer than the spectra of the heavy quarks. In the hadron interactions there is a similar way for the heavy quarks with relatively high p_T to fuse with the light antiquark from the same shower. However there exists an alternative possibility to recombine with the antiquark originating from another independent branch of the hadronization. Thus the produced meson spectra can differ from the spectrum of fragmentation mesons, in particular, can be more hard. This effect is discussed in detail e.g. in the paper¹⁵

2 Heavy quark production in k_T factorization

The cross sections of hard processes in hadron-hadron interactions is written in k_T factorization as the convolutions of the squared matrix elements of the sub-process calculated within the perturbative QCD with the parton distributions in the colliding hadrons,

$$\begin{aligned} \sigma_{pp} &= \frac{1}{64\pi^2} \frac{1}{s^3} \int d^4 p_1 d^4 p_2 \delta(x_1 y_1 s + p_{1T}^2 - m_Q^2) \delta(x_2 y_2 s + p_{2T}^2 - m_Q^2) \\ &\times d^2 q_{1T} d^2 q_{2T} \delta^{(4)}(q_{1T} + q_{2T} - p_{1T} - p_{2T}) \\ &\times \frac{\alpha_s(q_1^2)}{q_1^4} \frac{\alpha_s(q_2^2)}{q_2^4} f_g(y, q_{1T}, \mu) f_g(x, q_{2T}, \mu) |T(g^* + g^* \rightarrow Q + \bar{Q})|^2. \end{aligned} \quad (1)$$

The quarks momenta are decomposed here in Sudakov manner along the momenta of the protons, p_A and p_B , $p_A^2 = p_B^2 \simeq 0$, $2p_A \cdot p_B = s$, and the transverse momenta $p_{1,2T}$:

$$p_{1,2} = x_{1,2} p_B + y_{1,2} p_A + p_{1,2T}, \quad d^4 p_{1,2} = \frac{s}{2} dx_{1,2} dy_{1,2} d^2 p_{1,2T}. \quad (2)$$

The matrix element corresponds to the lowest order QCD gluon fusion amplitude $g^* + g^* \rightarrow Q + \bar{Q}$ taken for the off shell gluons, g^* , whose virtuality is due to their transverse momentum,

$$\begin{aligned} q_1 &= x_1^g p_B + y_1^g p_A + q_{1T} \simeq y p_A + q_{1T}, & q_2 &= x_2^g p_B + y_2^g p_A + q_{2T} \simeq x p_B + q_{2T}, \\ q_1^2 &\simeq q_{1T}^2, & q_2^2 &\simeq q_{2T}^2, & x &= x_1 + x_2, & y &= y_1 + y_2, \end{aligned} \quad (3)$$

$\alpha_S(q^2)$ is one loop running coupling constant, $\alpha_s(q^2) = 4\pi/(b \ln q^2/\Lambda^2)$, $b = 11 - 2/3n_f$, $\Lambda \simeq 0.25$ GeV. Like in the parton model the gluons are mainly aligned in the directions of the colliding hadrons, the light cone components $x_1^g \ll y_1^g$, $y_2^g \ll x_2^g$ are neglected in the amplitude, but the transverse momenta are no more negligible and play a central role in the k_T factorization formalism.

Though the incoming partons become virtual for non vanishing transverse momenta the hard scattering is gauge invariant at least at small x where k_T factorization works. If we take the gluon propagator $D^{\mu\nu}(q) = d^{\mu\nu}(q)/q^2$ in the planar gauge, $d^{\mu\nu}(q) = \delta^{\mu\nu} + (q^\mu n^\nu + q^\nu n^\mu)/q \cdot n$, the resulting amplitude turns out to be independent on the gauge fixing vector n^μ .⁹ The main contribution for the large invariant energy \sqrt{s} comes from $\delta^{\mu\nu}$ tensor, or more exactly, from its longitudinal part, so that $d^{\mu\nu}(q) \simeq 2/s(p_A^\mu p_B^\nu + p_A^\nu p_B^\mu)$. This form underlies the factorized expression (1), in which the incoming gluons have to be taken as purely longitudinal,

$$T(g^* + g^* \rightarrow Q + \bar{Q}) = \varepsilon^\mu(q_1) \varepsilon^\nu(q_2) T_{\mu\nu}(g^* + g^* \rightarrow Q + \bar{Q}), \quad \varepsilon(q_1) = p_A^\mu, \quad \varepsilon(q_2) = p_B^\mu.$$

Regarded as a part of the whole scattering the sub process amplitude is transverse,

$$(yp_A + q_{1T})^\mu T_{\mu\nu}(g^* + g^* \rightarrow Q + \bar{Q}) = 0, \quad (4)$$

and similarly for the second gluon. Due to this fact the longitudinal polarizations can be equivalently replaced with the transverse ones,^{9,14} $\varepsilon^\mu(q_1) = -q_{1T}^\mu/y$, $\varepsilon^\nu(q_2) = -q_{2T}^\nu/x$,

$$T(g^* + g^* \rightarrow Q + \bar{Q}) = \frac{q_{1T}^\mu}{y} \frac{q_{2T}^\nu}{x} T_{\mu\nu}(g^* + g^* \rightarrow Q + \bar{Q}), \quad (5)$$

but it allows for more general polarizations vectors,

$$\varepsilon_A^\mu = -\frac{1}{y}(q_{1T} - 2yp_A)^\mu, \quad \varepsilon_B^\nu = -\frac{1}{x}(q_{2T} - 2xp_B)^\nu. \quad (6)$$

All these forms are equivalent within k_T factorization accuracy owing to condition (4).

If the restrictions $|q_T| \ll |p_T|$ were valid for the all gluons' and quarks' momenta the matrix element would turn into the standard parton model expression for the real gluons, whereas the $q_{1,2T}$ integrals (5) in the cross section (1) recover averaging over their helicities. For $|q_T| \simeq |p_T| \gg m_Q^2$ the matrix element becomes much more complicated. It looks rather bulky and quite different from the parton model one.

There is a way, however, to modify the matrix element in a manner that drastically simplifies it making it closer to the standard parton model expression. To do it we note at first that $Q\bar{Q}$ pair can be produced in the kinematics (3) only if

$$s_{xy} = xys - |(q_{1T} + q_{2T})|^2 \gtrsim 4(m_Q^2 + |p_T|^2) \quad (7)$$

Assuming that in the integral (1) $x, y \ll 1$ and $x \sim y$ it is natural to conclude that for heavy quarks $y \gg |q_{1T}|^2/(ys)$, $x \gg |q_{2T}|^2/(xs)$ provided s is large enough. It allows to substitute in the relations (3) the light cone components with the values $x_1^g = -q_{1T}^2/(ys)$ and $y_2^g = -q_{2T}^2/(xs)$. These components still can be neglected in the matrix element thereby not affecting the k_T factorization validity. On the other hand they put the incoming gluons momenta on the mass shell. Moreover, the vectors (6) turn out to be the proper polarizations, $q_1 \cdot \varepsilon_A = 0$, $q_2 \cdot \varepsilon_B = 0$.

Thus having modified incoming momenta one arrives at the amplitude for the scattering of quasireal particles in the spirit of Weizsäcker-Williams method. Further, the amplitude of the real process remains unchanged after adding to the gluon polarization any vector proportional to its momentum. Using this freedom the two polarizations $\varepsilon_A, \varepsilon_B$ can be replaced with the equivalent ones $e_A/y, e_B/x$, such that $q_1 \cdot e_{A,B} = q_2 \cdot e_{A,B} = 0$. It brings the matrix element to the final form,

$$|T(g^* + g^* \rightarrow Q + \bar{Q})|^2 = \frac{2}{x^2 y^2 s_p^2} \frac{4 - 9z(1-z)}{3(1-z)^2 z^2} \quad (8)$$

$$\times \left\{ 4 [e_A \cdot e_B z(1-z) s_p + 2 e_A \cdot p_\perp e_B \cdot p_\perp]^2 + (1-z)z s_p^2 e_A \cdot e_B e_A \cdot e_B \right\}.$$

This is just the squared parton model Born amplitude $g + g \rightarrow Q + \bar{Q}$ except for it is not averaged over e_A, e_B polarizations. Here $s_p = 2 q_1 \cdot q_2$ is the pair invariant energy, p_\perp is the quark relative momentum, $p_\perp \cdot q_1 = p_\perp \cdot q_2 = 0$. The constraints $q_1 + q_2 = p_1 + p_2, p_1^2 = p_2^2 = m_Q^2$ are resolved for $q_{1,2}^2 = 0$ as

$$\begin{aligned} p_1 &= z q_1 + (1-z) q_2 + p_\perp, \quad p_2 = (1-z) q_1 + z q_2 - p_\perp, \\ d^4 p_1 d^4 p_2 \delta^{(4)}(q_1 + q_2 - p_1 - p_2) \delta(p_1^2 - m_Q^2) \delta(p_2^2 - m_Q^2) \\ &= \frac{1}{2} d p_\perp^2 dz \delta[|p_\perp|^2 - z(1-z)s_p - m_Q^2], \end{aligned}$$

leaving p_\perp as a single independent variable. The radial $|p_\perp|$ integral is convenient to do in terms of the variable z , ranging in the interval $(1-\rho)/2 \leq z \leq (1+\rho)/2$, $\rho^2 = 1 - 4m_Q^2/s_p$.

It is worth to point out that p_\perp is not orthogonal to the protons' momenta p_A and p_B . The conventional parton model kinematics looks like it is rotated with respect to the direction of the colliding protons in their center of mass frame.

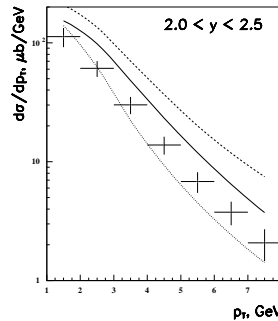


Figure 1: The cross section of c quark production at $\sqrt{s} = 7$ TeV in the rapidity interval $2 \leq y \leq 2.5$ calculated with 3 values of the factorization scale: $\mu^2 = m_c^2$, m_c is the c -quark mass, (dotted line), $\mu^2 = m_T^2$ (dashed line) and $\mu^2 = m_T^2/2$ (solid line), m_T is the c -quark transverse mass. The experimental points are taken from .²³

To make the "external" integrals over $x, y, q_{1,2T}$ the explicit expressions are needed:

$$e_A \cdot e_A = q_{1T}^2 = -|q_{1T}|^2, \quad e_B \cdot e_B = q_{2T}^2 = -|q_{2T}|^2, \quad e_A \cdot e_B = |q_{1T}||q_{2T}| \frac{[a b]}{s_p},$$

$$[a b] = \frac{1}{s_{xy}} \left[(q_{1T}^2 q_{2T}^2 + s_{xy}^2) \frac{q_{1T} \cdot q_{2T}}{|q_{1T}||q_{2T}|} - 2|q_{1T}||q_{2T}|s_{xy} \right],$$

$$s_p = \frac{1}{s_{xy}} [q_{1T}^2 q_{2T}^2 + s_{xy}^2 + 2 q_{1T} \cdot q_{2T} s_{xy}],$$

where s_{xy} is defined in (7). The cross section of the heavy quark pair production now reads

$$\begin{aligned} \sigma &= \frac{1}{16\pi s} \int \frac{dq_1}{q_1^4} \alpha_S(q_1^2) \frac{dq_2}{q_2^4} \alpha_S(q_2^2) \frac{dx}{x^2} \frac{dy}{y^2} dz d\phi d\theta \\ &\quad \times |T(g^* + g^* \rightarrow Q + \bar{Q})|^2 f_g(y, q_1, \mu) f_g(x, q_2, \mu). \end{aligned} \quad (9)$$

In this expression $q_{1,2} = |q_{1,2T}|$, the angle ϕ is defined as $q_{1T} \cdot q_{2T} = -|q_{1T}| |q_{2T}| \cos \phi$, the variable z and the angle θ represent the integral over p_\perp .

The integrals over small $q_{1,2T}$ reproduce averaging of the matrix element over gluon helicities occurring in the standard parton model. For the not small momenta they involve averaging over the orientations of the two dimensional plane where the parton model kinematics is relevant or, in other words, where the quarks' relative momentum p_\perp lies. In contrast to the conventional case it is not the plane orthogonal to the colliding hadrons, therefore the transverse quark momenta $p_{1,2T}$ in (2) are not directed along p_\perp . To pass to the center of mass frame for the colliding hadrons it suffices to reexpress p_A , p_B vectors through the momenta $q_{1,2}$ and the polarizations e_A , e_B .

The unintegrated parton distribution $f_g(x, q_T, \mu)$, entering the cross section (1), determines the probability to find a gluon initiating the hard process with the longitudinal momentum fraction x and the transverse momentum q_T . The factorization scale μ sets an upper momentum bound for the parton to be included into the distribution function. The partons carrying larger momenta have to be treated as participating in a rescattering, that gives rise to the NLO corrections or to the jet production etc. To find the function $f_g(x, q_T, \mu)$ on the basis of the conventional (integrated) gluon density $G(x, Q^2)$ we employ Kimber-Martin-Ryskin (KMR) approach^{16,17}

$$f_g(x, q_T, \mu) = T_g(q_T, \mu) \left[\frac{\alpha_S(q_T^2)}{2\pi} \int_x^\Delta P_{gg}(z) \frac{x}{z} G\left(\frac{x}{z}, q_T^2\right) dz \right], \quad (10)$$

where $P_{gg}(z)$ is the LO DGLAP gluon-gluon splitting function. It is singular for $z \rightarrow 1$, the singularity coming from the real soft gluon emission is regulated by the cutoff Δ . The singularity is canceled by the virtual loop corrections that are collected in the survival probability for the gluon to evolve untouched up to the factorization scale,

$$T_g(q_T, \mu) = \exp \left[- \int_{q_T^2}^{\mu^2} \frac{\alpha_S(p_T^2)}{2\pi} \frac{dp_T^2}{p_T^2} \int_0^\Delta P_{gg}(z) dz \right]. \quad (11)$$

The regulator is taken here as $\Delta = \mu / \sqrt{\mu^2 + q_T^2}$, the numerical results do not rather sensitive to its particular form.¹³ Since the main contribution comes to the integral

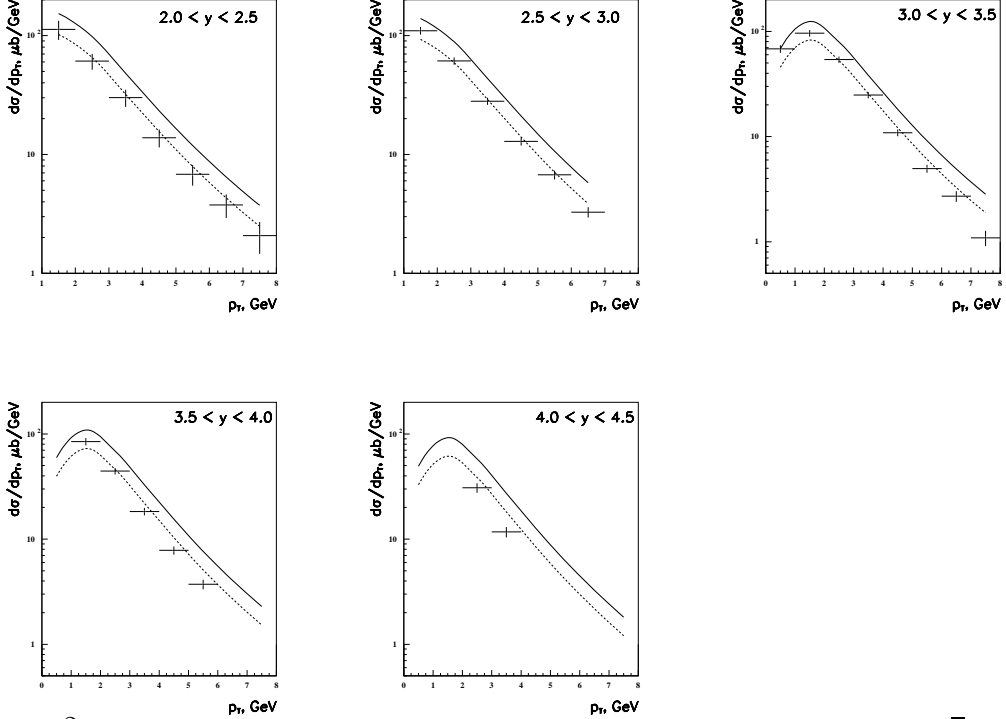


Figure 2: p_T dependence of the charm production in various rapidity regions at $\sqrt{s} = 7$ TeV. The solid curves are for the total charm production cross section, the dashed curves are for the charm meson production only. The experimental data are taken from.²³

(10) from $z \sim 1$ we put in the integrand $x/z g(x/z, q_T^2) \approx xg(x/z, q_T^2)$ to avoid too singular behavior at $z \sim 0$.

The structure functions are unknown in the infrared domain of the small momenta $q_{1,2T}^2$. That is why the contributions from $|q_{1,2T}^2| < Q_0^2$ and $|q_{1,2T}^2| > Q_0^2$, $Q_0^2 \sim 1$ GeV², are calculated separately. When $|q_T^2| < Q_0^2$ the unintegrated distribution is replaced with the usual structure function, $f_g(x, q_T, \mu) = xG(x, Q_0^2)T(Q_0, \mu)$, multiplied by the survival probability $T(Q_0, \mu)$ not to have transverse momenta larger than Q_0^2 (see¹³). The parametrization¹⁸ having a rather simple analytical form is taken for the gluon structure function $G(x, Q^2)$.

3 Comparison with the experimental data

We start from the data on the charm production obtained at the LHC at the energy $\sqrt{s} = 7$ TeV because they contain the cross sections of the production of charm D^0 , D^+ , D_s^+ mesons together with Λ_c^+ baryon. It makes it more suitable to compare with

since the produced c quark can fragment into the mesons as well into the baryons.

There are two basic parameters in the calculation – the mass of the heavy quark and the factorization scale. We take the same c and b masses as in our previous paper:¹³

$$m_c = 1.4 \text{ GeV}, \quad m_b = 4.6 \text{ GeV}.$$

The factorization scale μ^2 separates the partons participating in the process from those responsible for the evolution of the structure function. It should be taken to be of the order of the typical hardness of the reaction. The role of μ^2 becomes more important at high energies in the small x region, where the structure function grows.

The cross section $d\sigma/dp_T$ of c quark production calculated at $\sqrt{s} = 7$ TeV in the rapidity interval $2 \leq y \leq 2.5$ are presented in Fig. 1 for three different values of the factorization scale: $\mu^2 = m_c^2$, $\mu^2 = m_T^2$ and $\mu^2 = m_T^2/2$, where p_T is the quark transverse momenta, $m_T^2 = m_c^2 + |p_T|^2$. The curve for $\mu^2 = m_T^2$ is seen to decrease with p_T too slow while for $\mu^2 = m_c^2$ it decreases too fast so almost everywhere it lies below the data also shown in the Fig. 1. The curve with $\mu^2 = m_T^2/2$ better fits the data. It has roughly the same slope though goes uniformly above the experimental points. It is the value $\mu^2 = m_T^2/2$ that has been taken for the further calculations.

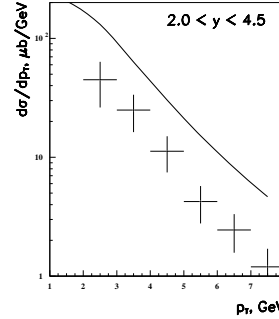


Figure 3: The cross section of Λ_c baryon production at $\sqrt{s} = 7$ TeV in the rapidity interval $2 \leq y \leq 4.5$. The experimental data are taken from.²³

The factorization scale significantly controls in what extent the parton rescattering affects the calculation output for a given scheme. Thus the choice of μ^2 not only influences the perturbative NLO corrections but may help to achieve the better description of the hadronization stage.

The normalization exceeding of the calculated results above the experiment can be explained by the fact that only the charm mesons D^0 , D^+ , D_s^+ are mostly detected while the c quark production implies the subsequent fragmentation also into the charm

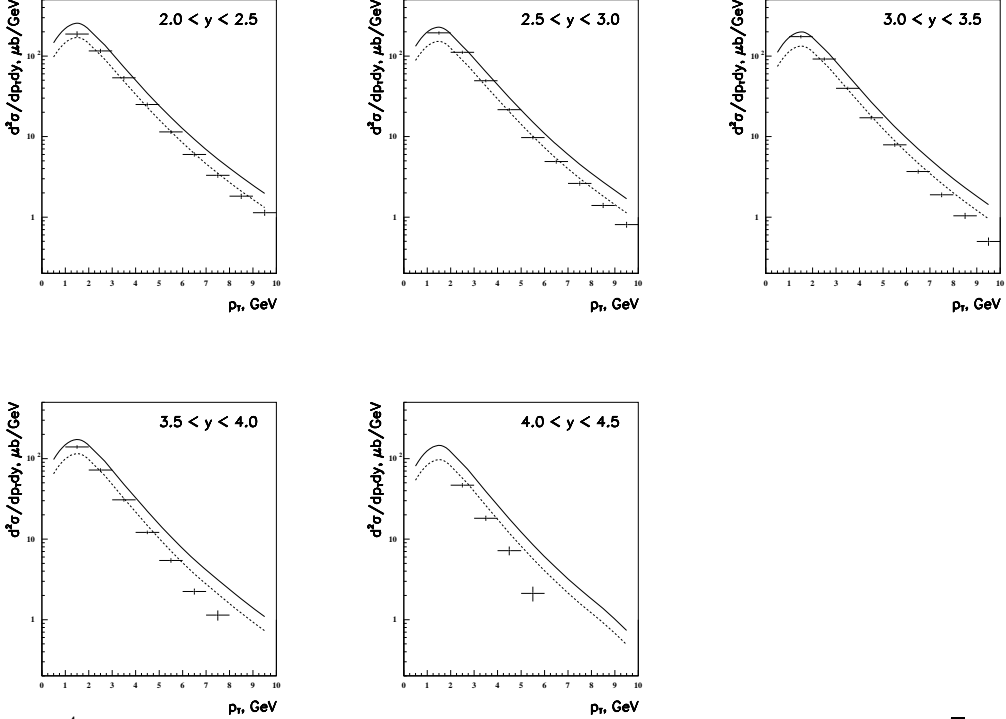


Figure 4: p_T dependence of the charm production in various rapidity regions at $\sqrt{s} = 5$ TeV. The solid curves are for the total charm production cross section, the dashed curves are for the charm meson production only. The experimental data are taken from.²⁴

baryons such as Λ_c etc. To estimate the correct normalization one can employ the simple quark combinatorics.^{19,20} Assuming^{19,20} the same probabilities for the charm quark to couple with a quark or antiquark one gets after the first fusion

$$c + (1/2 q + 1/2 \bar{q}) \rightarrow 1/2 c q + 1/2 M_c.$$

Then the second fusion gives

$$1/2 c q + (1/2 q + 1/2 \bar{q}) \rightarrow 1/4 B_c + 1/4 c + 1/4 M,$$

where M_c , B_c are the charmed meson and baryon, M is the sea meson. Thus the charmed mesons and baryons should be produced in the proportion 2:1, that is

$$c \rightarrow 2/3 M_c + 1/3 B_c. \quad (12)$$

As was shown in Ref²¹ this relation is in reasonable agreement with the experimental data obtained in e^+e^- annihilation. However the multiplicity of secondary baryons is significantly smaller than 1/3 for the pion nucleon collisions.²² Nevertheless we use

the ratio (12) as an upper boundary for baryon production for the absence of another theoretical models.

In all the following figures we show the results for c quark production by the solid curves and the results for the charmed meson production estimated according to eq.(12) by the dashed curves.

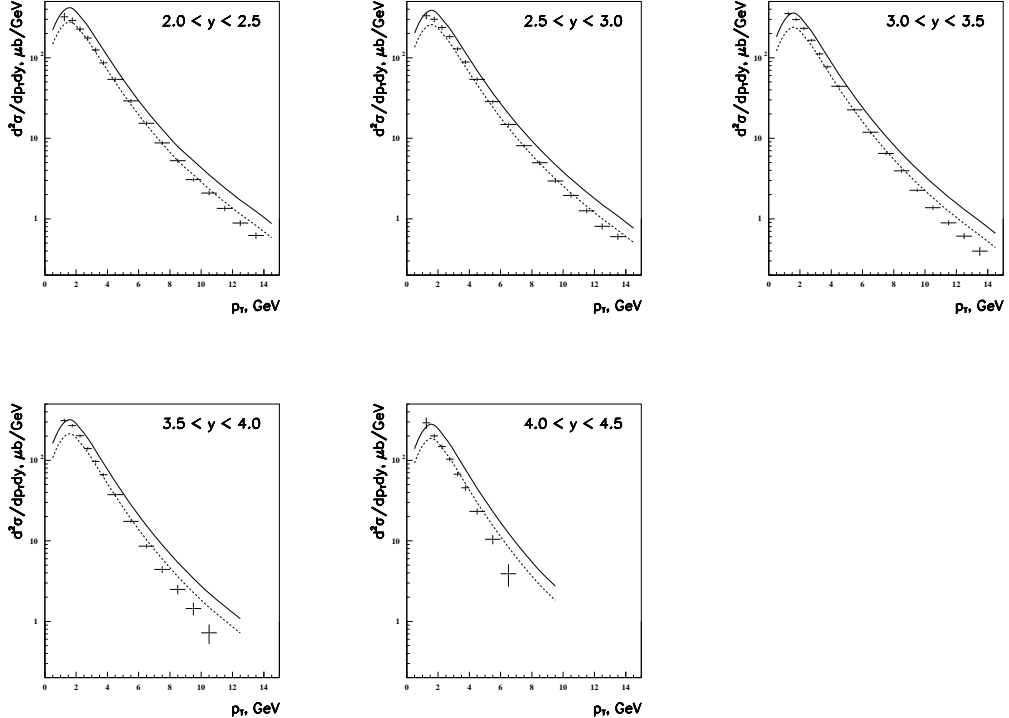


Figure 5: p_T dependence of the charm production in various rapidity regions at $\sqrt{s} = 13$ TeV. The solid curves are for the total charm production cross section, the dashed curves are for the charm meson production only. The experimental data are taken from.²⁵

The comparison with the experimental data on p_T dependence of charm production at $\sqrt{s} = 7$ TeV in various rapidity intervals are presented in Fig. 2. The solid curves are higher than the experimental points but the dashed curves for the charm meson production are in reasonable agreement in all cases. Some discrepancy at the large rapidities can be explained by overestimated small x region in the GRS structure function.¹⁸

To check up the ratio of the charmed meson/baryon outcome the experimental data on Λ_c production at 7 TeV are presented in Fig. 3 together with our results for the charm baryon production estimated as 1/3 of the total one. The evaluated curve is higher than the experimental points. A possible reasons could be in another undetected charm hadrons or in a violation of the quark combinatorics.

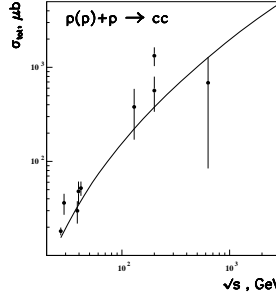


Figure 6: Total cross section of charm production in pp and $\bar{p}p$ collisions. The experimental points are taken from.^{26–31}

There also exist the experimental data for the charm mesons production at 5 TeV and 13 TeV as the functions of p_T in various rapidity regions. They are compared with our calculations in Fig. 4 and Fig. 5. Again the dashed curves demonstrate reasonable agreement with the data at the both energies.

Our calculation scheme yields the reasonable values for the total charm production cross section at the lower energies. They are shown in Fig. 6.

The results of our approach extended within the same assumptions to the beauty production are presented in Fig. 7. They show the smaller than 1/3 probability for the b quark to fragment into baryons. Thus the cross section of B meson production is perhaps closer to the total cross section of b quark production.

The beauty production at the lower energy is also satisfactorily reproduced as is shown in Fig. 8, where the cross section of b quark production for $p_T > p_T^{\min}$ and $|y| < 1$ is presented as a function of p_T .

4 Conclusion

We have demonstrated that the k_T factorization method admits reformulation in a manner making it similar to the conventional parton model. Likewise in the parton model the sub process amplitude is written here for on shell partons. The integral over the transverse momenta of the incoming off shell gluons, which is the main ingredient of the k_T factorization, turns here into the integral over the orientation of the plane, where the incoming parton momenta lie. The effect of this integrals, that recovers the substantial part of the NLO parton model, rapidly grows with the energy. Their relative weight in the total cross section at $\sqrt{s} = 27$ GeV is about 40%, the rest comes from the transverse momenta $|q_T^2| < Q_0^2$ corresponding to the conventional LO parton

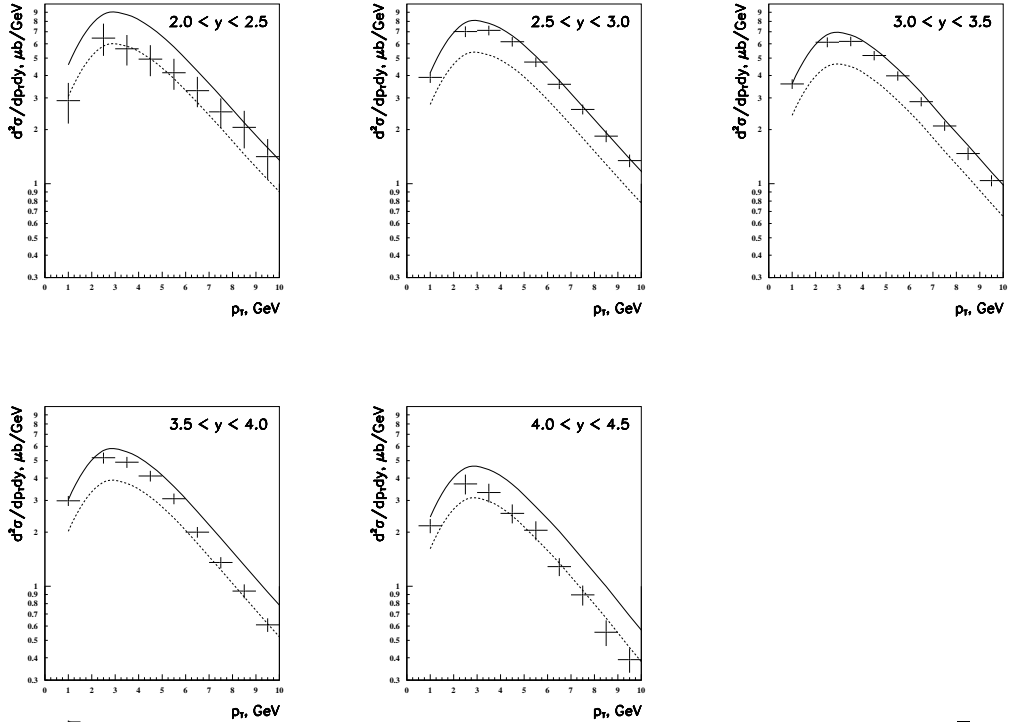


Figure 7: p_T dependence of the beauty production in various rapidity regions at $\sqrt{s} = 7$ TeV. The solid curves are for the total beauty production cross section, the dashed curves are for the beauty meson production only. The experimental data are taken from.³³

model. At the same time the LO parton model gives only 10% at $\sqrt{s} = 7$ TeV, so that the k_T factorization contribution dominates at this energy.

Assumptions made to modify the k_T factorization formalism seem to be rather natural and not too restrictive. The numeric calculations confirm that they are sufficient for quite reasonable description of the data.

As a rule our solid curves are slightly above the experimental points. Most probably it is the consequence of the fact that the produced heavy quarks can fragment both into mesons and baryons whereas the experiment data are presented mainly for the secondary mesons. The outcome meson/baryon ratio is close to 1/3 for the c quark production in accordance with a simple quark combinatorics, (of course we can not say that 1/3 agrees with the data better than, say, 1/5) while this value is clearly overestimated for the b quark case.

To summarize, a large variety of experimental data have been reproduced at least qualitatively with two parameters, that is the mass of the heavy quark and the factorization scale. As the masses can not be varied in a wide ranges it leaves only one actual parameter, which allows nevertheless to obtain a reasonable description of the

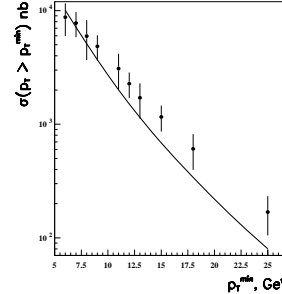


Figure 8: The calculated results for b quark production cross section $\sigma(p_T > p_T^{\min})$ at $\sqrt{s} = 1.8$ TeV and $|y| < 1$. The experimental data are taken from³²

experimental data both for charm and beauty production at different energies.

The authors are grateful to M.G. Ryskin for helpful discussion.

References

- [1] P.Nason, S.Dawson and R.K.Ellis. Nucl. Phys. **B303** (1988) 607.
- [2] G.Altarelli, M.Diemoz, G.Martinelli, P.Nason. Nucl. Phys. **B308** (1988) 724.
- [3] P.Nason, S.Dawson and R.K.Ellis. Nucl. Phys. **B327** (1989) 49.
- [4] Y. L. Dokshitzer, D. Diakonov and S. I. Troian, Phys. Rept. **58**, 269 (1980).
- [5] E.A.Kuraev, L.N.Lipatov, V.S.Fadin. Sov. Phys. JETP **45** (1977) 199.
- [6] I.I. Balitsky and L.N. Lipatov, Sov. J. Nucl. Phys. **28**, 822 (1978).
- [7] L.V. Gribov, E.M. Levin and M.G. Ryskin, Phys. Rept. **100 (1983)** 1.
- [8] E.M. Levin, M.G. Ryskin, Yu.M. Shabelski and A.G. Shuvaev, Sov. J. Nucl. Phys. **53** (1991) 657.
- [9] S. Catani, M. Ciafaloni and F. Hautmann, Nucl. Phys. **B 366** (1991) 135.
- [10] J.C. Collins and R.K. Ellis, Nucl. Phys. **B 360** (1991) 3.
- [11] V.F.Saleev and N.P, Zotov, Mod. Phys. Lett. A9 (1994) 151; A11 (1996) 25.
- [12] S.P. Baranov and M. Smizanska, Phys.Rev. D62 (2000) 014012.

- [13] Y. M. Shabelski and A. G. Shuvaev, Phys. Atom. Nucl. **69** (2006) 314 [hep-ph/0406157].
- [14] M. G. Ryskin, A. G. Shuvaev and Y. M. Shabelski, Phys. Atom. Nucl. **64** (2001) 1995 [Yad. Fiz. **64** (2001) 2080] [hep-ph/0007238].
- [15] A.K.Likhoded and S.R.Slabospitsky. Phys. Atom. Nucl. **60** (1997) 981; 62 (1999) 693; hep-ph/0008230.
- [16] M.A. Kimber, A.D. Martin and M.G. Ryskin, Phys. Rev. **D 63** (2001) 114027 [hep-ph/0101348].
- [17] G. Watt, A.D. Martin and M.G. Ryskin, Eur. Phys. J. **C 31** (2003) 73 [hep-ph/0306169].
- [18] M. Gluck, E. Reya and A. Vogt. Z.Phys. C67 (1995) 433.
- [19] V. V. Anisovich and V. M. Shekhter, Nucl. Phys. B **55**, 455 (1973) Erratum: [Nucl. Phys. B **63**, 542 (1973)]. doi:10.1016/0550-3213(73)90391-X, 10.1016/0550-3213(73)90163-6
- [20] V. V. Anisovich, Sov. J. Nucl. Phys. **28** (1978) 390 [Yad. Fiz. **28** (1978) 761].
- [21] Anisovich V.V, Volkovitsky P.E. and Kobrinsky M.N. Yad. Fiz. **29** (1979) 1054
- [22] Shabelski Yu.M. Yad. Fiz. **33** (1981) 1379
- [23] R. Aaij *et al.* [LHCb Collaboration], Nucl. Phys. B **871** (2013) 1 [arXiv:1302.2864 [hep-ex]].
- [24] R. Aaij *et al.* [LHCb Collaboration], JHEP **1706** (2017) 147 [arXiv:1610.02230 [hep-ex]].
- [25] R. Aaij *et al.* [LHCb Collaboration], JHEP **1603** (2016) 159 Erratum: [JHEP **1609** (2016) 013], JHEP **1705** (2017), 074, [arXiv:1510.01707 [hep-ex]].
- [26] C. Lourenco and H. K. Wöhri. Phys. Rept. **433** (2006) 127.
- [27] M. C. Abreu et al., NA38 and NA50 Collaborations. Eur. Phys. J. C **14** (2000) 443.
- [28] O. Botner et al., UA2 Collaboration. Phys. Lett. **B236** (1990) 488.
- [29] K. Adcox *et al.* [PHENIX Collaboration], Phys. Rev. Lett. **88** (2002) 192303 [nucl-ex/0202002].

- [30] A. Adare *et al.* [PHENIX Collaboration], Phys. Rev. Lett. **97** (2006) 252002 [hep-ex/0609010].
- [31] J. Bielcik [STAR Collaboration], nucl-ex/0606010.
- [32] B. Abbott *et al.* [D0 Collaboration], Phys. Lett. B **487** (2000) 264 [hep-ex/9905024].
- [33] R. Aaij *et al.* [LHCb Collaboration], JHEP **1308** (2013) 117 [arXiv:1306.3663 [hep-ex]].